Tom Plazek
4284678
Due: 11/30/22

Analyzing Mt. Kilauea Using TIR and SAR Data

1. Abstract

The purpose of this report was to explore the areas in and around the volcano of Kilauea in Hawai'i using thermal infrared (TIR) and Airborne Synthetic Aperture Radar (AIRSAR) data. Polarizations in the C, L and P radar bands allowed for surface roughness to be observed and calculated. These surface roughness's and polarizations helped to determine the relative age of the Kilauea lava flows. Rayleigh equations were used to determine the rough and smooth criteria and were used to estimate the surface roughness on the HH polarization. Younger flows were picked up by the shorter wavelengths and older flows were picked up by the longer wavelengths. This was due to their relative roughness and the wavelengths' ability to scatter off of smaller or larger particles.

2. Introduction

Kilauea has covered nearly 90% of its surfaces in basaltic lava flows in the past 1,000 years. Changes in Kilauea can be observed over time, even within short time periods. The imagery used was captured by the Advanced Spaceborne thermal Emissions and Reflection Radiometer (ASTER), along with AIRSAR. Radar data allows for different polarizations to be observed, which can be useful for indicating shapes and surface roughness's. The polarizations which this lab focused on were the HH, HV and VV polarizations. HH polarizations in the C, L and P bands, alongside Rayleigh criteria results, were used to calculate a surface roughness for the HH polarization in each of the bands. Additionally, color composited made with like polarizations, along with USGS flow maps were used to analyze the volcanos lava flows over the past century. Finally, two Digital Elevation Models (DEM) of Kilauea, created using ASTER imagery from 2015 and 2021 were analyzed. The models were created to depict the difference in crater conditions after a 2018 eruption. After the eruption in 2018, the crater increased in both volume and height.

3. Methods

3.1 Initial Analysis

This work required both ASTER and AIRSAR data for analysis. All imagery was processed using ENVI. Initially, the ASTER data was loaded in via band 12 and a preliminary visual analysis was performed.

3.2 TIR Analysis

A decorrelation stretch was performed on bands 14, 12 and 10. This stretch was subsequently opened using the same band combination as a R, G, B color composite. The lava flows were observed in this stretch to determine their geologic composition. (Figure 1)

3.3 SAR Pulse Duration Calculation

Using the look angle found in the ENVI header data, the pulse duration of the instrument was calculated using the following equation:

$$R_r = \left(\frac{c * t}{2} 2\cos(\alpha)\right)$$

Where R_r is the range resolution, c is the speed of light and t is the pulse duration. The equation can be rearranged to solve for t:

$$t = \left(\frac{2 * \frac{R_r}{2\cos(\alpha)}}{c}\right)$$

3.4 AIRSAR Data Analysis

AIRSAR data in nine different polarization bands was loaded into the software one at a time for visual analysis. Particular attention was paid to the HH and HV polarizations (Figures 2, 3). The radar illumination direction was determined and the crater shadow in pixel 300,360 was measured. Additionally, the height of the volcano was determined using the measured distance and look angle of the data. The angle information was provided in the header.

3.5 Rayleigh Criteria Calculations for Surface Roughness

Using the HH polarization in the C, L and P bands, the surface smoothness and roughness criteria were calculated using the following equations:

Smoothness equation $\Lambda h < \frac{\lambda}{8\sin(\Theta)}$

Roughness equation $\Lambda h > \frac{\lambda}{4.4\sin(\Theta)}$

3.6 Calculating HH Polarization Surface Roughness

Assuming that there was a linear relationship between 0 DN value for smooth and 255 DN value for rough, the surface roughness of the HH polarization was calculated. This was achieved by using this series of equations:

$$HH_R = (Smooth - Rough) = X$$

$$\frac{X}{255} = X`$$

$$X` * DN_{Measured} = HH_R$$

3.7 Comparing Data with Google Earth and USGS

The like polarizations for each band were placed into a color composite image and compared to the same location on Google Earth and against a USGS lava flow map with dates. The HH and HV color composites were analyzed further to investigate visual anomalies in their imagery.

3.8 ASTER Derived DEM Analysis

The 2015 and 2021 DEM's were loaded into ENVI in two separate displays. After linking the displays, a transect was drawn across both of the calderas. Additionally, the radius of each caldera was measured. Using this information, the volume of the two calderas was measured using the following equation for a cylinder:

$$V = \pi r^2 * h$$

The height was derived from the spatial profiles of the datasets. This spatial profile was generated from the transect taken from each dataset.

4. Results and Analysis

4.1 Initial and TIR Analysis

Upon performing the first decorrelation stretch, the different colors were determined to be lava flows of different composition and weathered states. Hawaiian lava flows contain more labradorite and olivine than quartz, and the TIR spectra seemed to indicate high reflectiveness. Materials like olivine are more reflective due to their glass-like composition.

4.2 SAR Pulse Duration Calculations

The pulse duration calculated using the equation listed above was determined to have a value of $3.14 * 10^{-8}$ seconds or 0.0314 microseconds. Pulse durations refer to the time from the beginning of one pulse to the beginning of the next.

4.3 Rayleigh Criteria Calculations for Surface Roughness

Using the Rayleigh equations given above, the smooth and rough thresholds were calculated for the HH polarization. (Table 1)

4.4 Calculating HH Polarization Surface Roughness

Using the equations above, the surface roughness was estimated for the HH polarizations (Tables 2, 3). It was determined that the wavelength roughness appears to change since shorter wavelengths have the ability to interact with and reflect off of smaller particles. The opposite is true for longer wavelengths.

4.5 Comparing Data with Google Earth and USGS

The color composites revealed the ages of certain lava flows on and around the crater. The shortest bands indicated the youngest lava flows and the longest bands indicated the oldest lava flows. Young lava flows are short than old ones, so the shortest wavelengths were able to interact with the smaller smooth particles, while the longer wavelengths interacted with the roughest particles. The USGS map, along with the polarizations can be view below. (Figures 4, 5, 6, and 7).

4.6 ASTER Derived DEM Analysis

Using the spatial profile and the equation listed above, it was determined that the volume of the 2015 crater was 0.0609 km^3 and the volume of the 2021 crater was calculated as 0.950 km^3. Additionally, the white area of elevation adjacent to the caldera post eruption was postulated to be a newly formed lava dome as a result of the 2028 eruption. (Figures 8, 9)

5. Conclusions

Remote sensing is one of the most effective ways to study volcanos. Polarizations can be a useful tool in determining surface roughness's when working with RADAR data. The polarization color composites were also useful in determining the geologic makeup of the lava flows from Kilauea over time. Rougher surfaces indicated older flows, while smooth surfaces indicated younger flows. Additionally, DEM's derived from remotely sensed images proved to be useful for determining change in height over time, along with calculating the volumes of surface points of interest.

6. References

Airborne Synthetic Aperture Radar (AIRSAR) | NASA Airborne Science Program. (n.d.). https://airbornescience.nasa.gov/instrument/AIRSAR

Polarization in radar systems. (n.d.). https://www.nrcan.gc.ca/maps-tools-and-publications/satellite-imagery-and-air-photos/satellite-imagery-products/educational-resources/tutorial-radar-polarimetry/polarization-radar-systems/9567

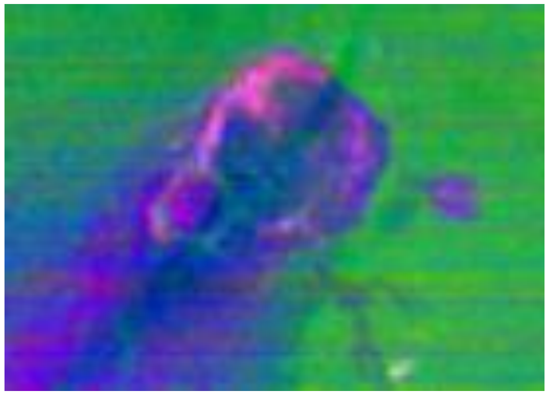

Figure 1 – Centered over Kilauea caldera crater

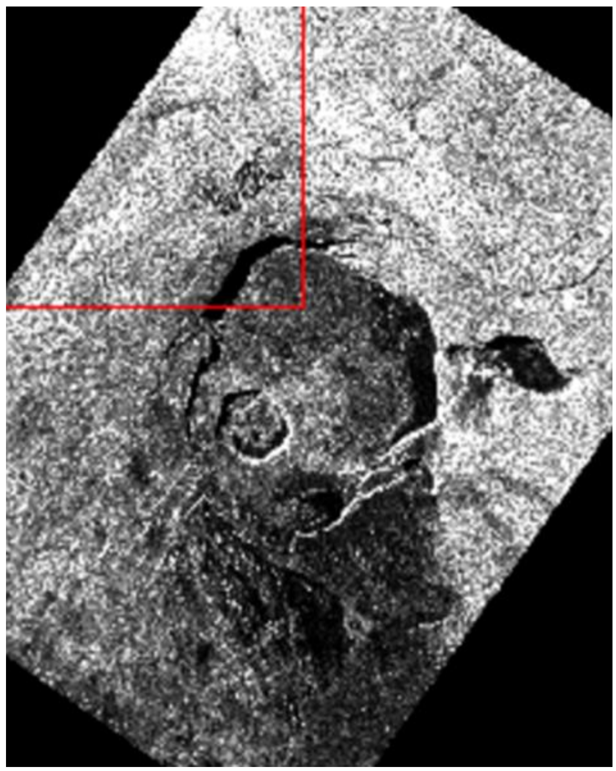

Figure 2 – HH polarization of Mt. Kilauea derived from AIRSAT data

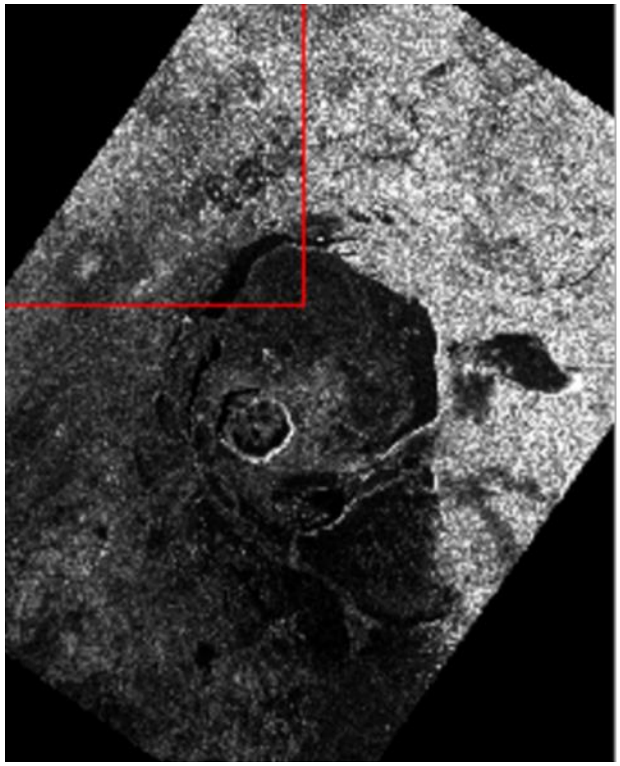

Figure 3 – HV polarization of Mt. Kilauea derived from AIRSAT data

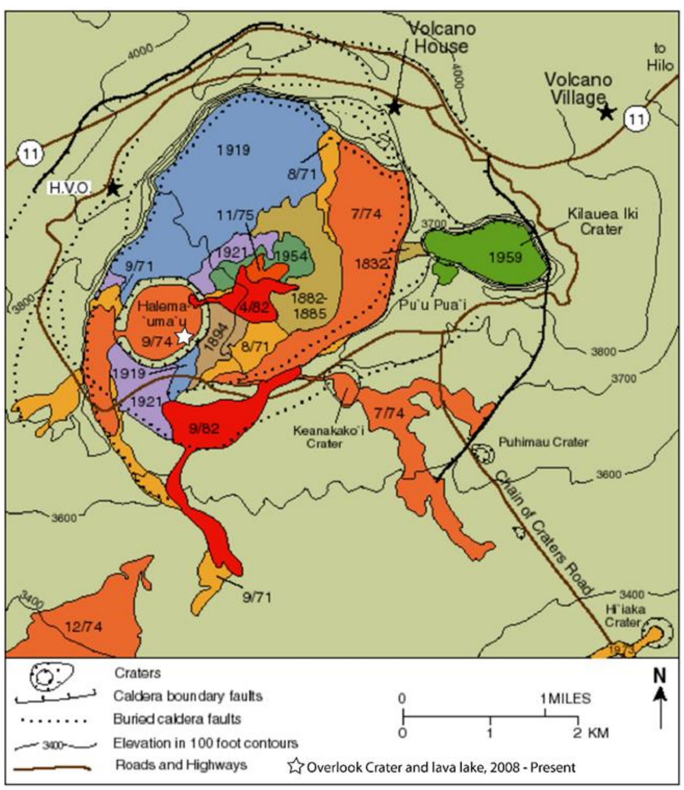

Figure 4 – Time stamped USGS lava flow map for Mt. Kilauea.

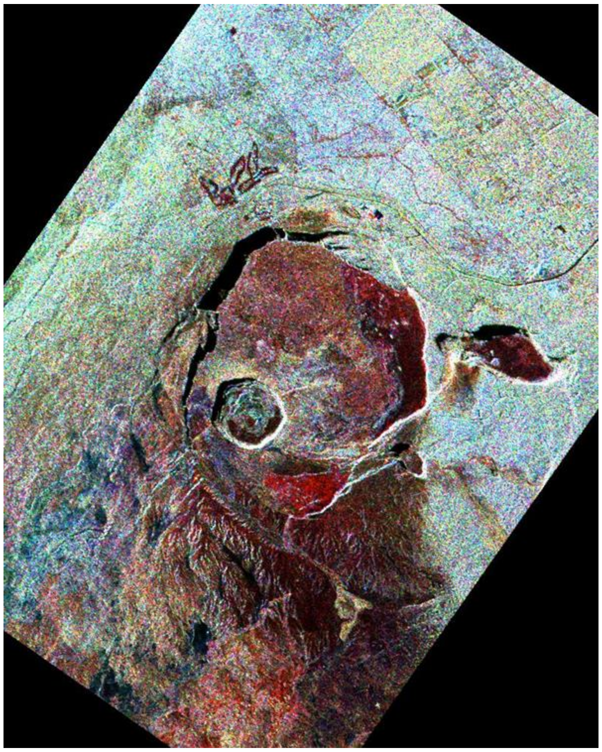

Figure 5 – HH polarization of Kilauea (AIRSAT)

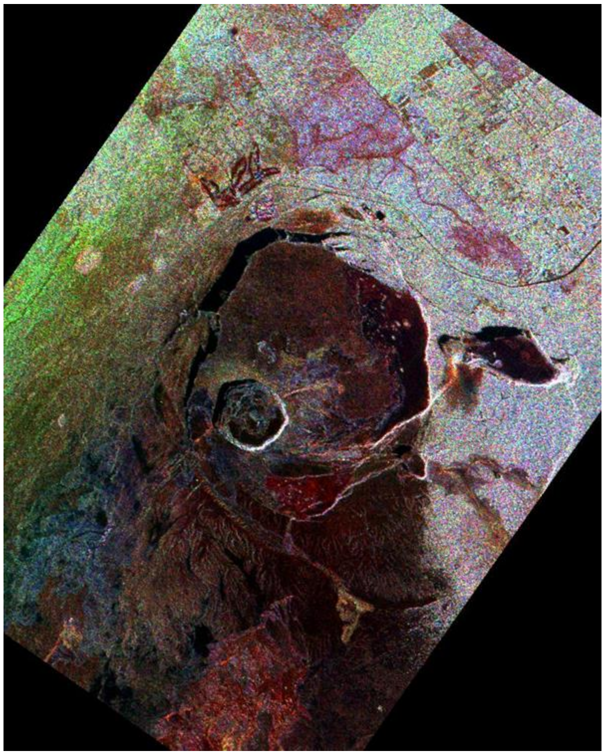

Figure 6 – HV polarization of Mt. Kilauea (AIRSAT)

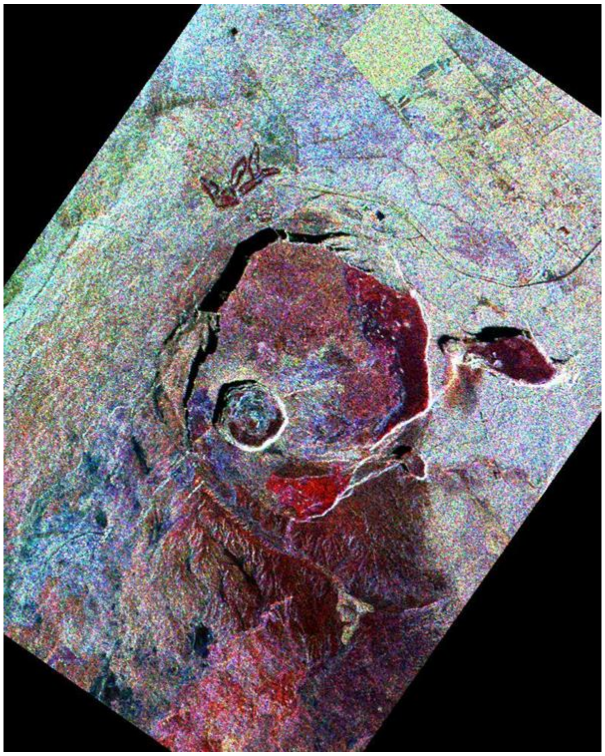

Figure 7 – VV polarization of Mt. Kilauea (AIRSAT)

Figure 8 – 2015 DEM of Kilauea derived from ASTER data

Figure 9 – 2021 DEM of Kilauea derived from ASTER data

HH polarization bands	Smooth if **Δh <**	Rough if **Δh >**
C	1.01	1.83
L	4.07	7.39
P	11.8	21.5

Table 1 – Calculated Rayleigh Values

HH polarization band:	Measured DN:	Surface Roughness (cm):
C	233	0.749
L	190	2.47
P	101	3.84

Table 2 – HH polarization surface roughness estimates for pixel 442, 445

HH polarization band:	Measured DN:	Surface Roughness (cm):
C_{hh}	211	0.678
L_{hh}	48	0.625
P_{hh}	39	1.48

Table 3 – HH polarization surface roughness estimates for pixel 430, 666